Proceedings of the 28th IEEE
EMBS Annual International Conference
New York City, USA, Aug 30-Sept 3, 2006

Sub-second functional imaging by Electrical Impedance Tomography

H. McCann[1], N. Polydorides[2+], J.C. Murrieta-Lee[1++], Kou Ge[1+++], P. Beatty[3], and C.J.D. Pomfrett[3]

[1] School of Electrical & Electronic Engineering, [2] School of Mathematics, [3] School of Medicine, Univ. of Manchester, UK
[+]Now at the Univ. of Cyprus, Nicosia, Cyprus. [++]Now at ITSON, Sonora, Mexico [+++]Visitor from Nanjing Univ. of Science & Technolgy, PR China

Abstract—**Functional imaging of the human brain using Electrical Impedance Tomography (EIT) is reported, where the measurement data were collected over a period of 308ms. Initiation of the measurement sequence occurred at times ranging from 70 to 740 ms after administration of visual or auditory stimuli to two volunteers. The reconstructed images of conductivity change due to individual visual stimulus events correspond with anatomical regions known to be involved in visual sensory processing and the processing of cognitive reflexes. We propose that the mechanism enabling this EIT imaging capability is concerned with synaptic effects upon local conductivity of bulk brain tissue, which is supported by the observations of Klivington and Galambos[1]. In turn, the sensitivity of EIT to this effect is much greater than previously expected [2], due to the high conductivity of in-vivo skull [3].**

Keywords—**Scalp, skull, brain, conductivity, function, fast, electrical, impedance, tomography, imaging**

I. INTRODUCTION

To date, no functional imaging technique for the human brain provides the combination of (a) full depth sensitivity, (b) sub-second temporal resolution, and (c) portability. Direct electrical measurement gives excellent temporal resolution, but the haemodynamic response of the brain takes about 5 seconds to occur after stimulus. EIT is a candidate technique for direct functional brain imaging through its sensitivity to conductivity variations within the measurement subject; it has potential for fast measurements over periods much less than 1s. Holder and co-workers have demonstrated [4] encouraging imaging capability by EIT, with a frame acquisition time of 25s; stimuli were applied repeatedly to the patient, at a much faster rate than the imaging rate, for several minutes while EIT data were gathered. The observed effects are attributed to the haemodynamic mechanism. Invasive studies on animals [5,6] show that, concerning the direct observation of the brain's electrical activity, the relevant temporal domain extends down to about 10 ms.

We have previously reported [7] measurements of EIT voltages under visual and auditory stimulus, compared to non-stimulus conditions. Using the same raw data, we report here on the images of conductivity change that occur on stimulus, analyzing them in terms of their compatibility with expected neural processes in response to the stimuli. Lastly, we propose a mechanism that would account for our observations.

II. METHODOLOGY

A. Experimental

The volunteer experiments are described in detail in [7]. The procedure is summarised briefly here. The volunteers were fully awake throughout the tests. Visual stimulus consisted of a 50ms flash of red light over the whole field of view; the auditory stimulus consisted of 75 dB SPL binaural clicks. Prior to stimulation of each volunteer, control ("reference") EIT and EEG datasets were recorded.

The 16 EIT electrodes (Aspect Medical Systems *ZipPrep*) were mounted directly onto the scalp in a plane that was chosen to be an axial section through the *superior putamen* (Fig. 1), i.e. optimized for measuring the brain's visual processing. Polar current patterns (sinusoidal, 1 mA peak-to-peak, 9.6 kHz) were driven between opposite EIT electrodes and the in-phase voltage was measured between all other nearest-neighbour electrodes. Electrode 14 was inoperative. A complete frame of data consists of 72 measurements. The total time for the EIT system to acquire a single frame of data was 308.1ms. The electrode contact impedance is dominated by the capacitive component, which occasionally results in voltage-pair measurements being corrupted. This was minimized by using low voltage-gain, with resulting voltage resolution 0.48mV. Corrupted data have been excluded from the analysis below, exploiting their clear signature.

When stimulus frames are gathered, the period between application of stimuli is pseudo-randomised (average 1 Hz) in order to avoid brain habituation. A further pseudo-

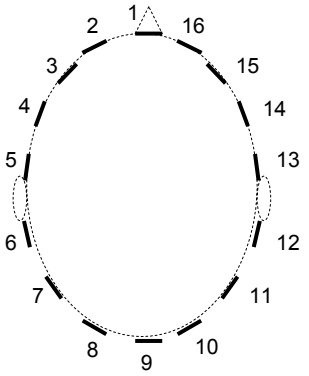

Fig. 1. EIT electrode layout.

randomised 'latency' delay t_ℓ (70 - 740 ms) is imposed between application of the stimulus and the initiation of the EIT measurement sequence. EEG voltages during the latency period are entirely as expected (max. about 5μV), and they go off-scale at the end of the latency period due to the EIT current injection. For each volunteer, under each condition, typically 50 – 58 frames are used in the analysis.

B. Analytical

Simple statistical techniques were used to study the behaviour of the voltage measurements V_{ij} between electrode-pairs (i,j) under various conditions [7]. For each volunteer under given conditions, we have analysed the distribution and mean value (denoted $<V_{ij}>$) of these data, for each current injection pattern, over a set of EIT frames (typically 50 – 58 frames). The change $\Delta<V_{ij}>$ in the mean value between no-stimulus and stimulus conditions has been analysed (equ. (1)). The standard error on $\Delta<V_{ij}>_{stim}$ (denoted $\delta\Delta_{ij}$) has a minimum value of 0.20mV due to the voltage resolution.

$$\Delta<V_{ij}>_{stim} = |<V_{ij}>_{ref}| - |<V_{ij}>_{stim}| \qquad (1)$$

$$\nabla.(\sigma\nabla u) = 0 \qquad (2)$$

The "dynamic imaging" strategy is adopted, where images are reconstructed from the differences (δy) in pair voltages between, on the one hand, a frame obtained under stimulus, and on the other hand a reference frame consisting of the no-stimulus mean values $<V_{ij}>_{ref}$. An image of the *change* of conductivity due to stimulus, δσ is thus produced for each stimulus frame. Equ. (2) describes the dependence of the potential *u* on the domain of interest in terms of the conductivity distribution σ. The method described in [8] was used to calculate the forward solution for δy. The forward map F: $\sigma \rightarrow y$ is subsequently linearised at the reference values σ_0, yielding the matrix A that satisfies equ. (3). The forward map F is non-injective and its first-order derivative A (the Jacobian matrix) is a linear compact operator with exponentially decaying singular values, hence severely ill-conditioned. The solution for δσ is calculated by finding the minimum of the Lagrangian function T given by equ. (4), where $\|x\|$ is the 2-norm of a vector x, λ is a strictly positive constant, and D is a smoothing operator which expresses the expected degree of smoothness in δσ and hence the fact that, with a small number of measurements for each frame, our solution is not sensitive to sharp spatial variations in conductivity.

$$A(\delta\sigma) = \delta y \qquad (3)$$

$$T(\delta\sigma,\lambda) = \frac{1}{2}\|A(\sigma_0)\delta\sigma - \delta y\|^2 + \lambda\|D\delta\sigma\|^2 \qquad (4)$$

The value of λ controls the influence of the experimental data upon the resultant δσ images, against that of the prior information. The value $\lambda = 10^{-2}$ was estimated by repetitive forward computations to find the optimum matching between Aδσ and δy. This procedure is equivalent to the well-known generalized Tikhonov regularization method [8]. The 17584 elements of the scalp and the 11981 elements of the skull [8] were each fixed at their nominal conductivity and not included in the 3D inverse problem solution.

III. RESULTS AND ANALYSIS

A. Voltage data

As previously reported [7], the patterns of our results for $<V_{ij}>_{ref}$, i.e. without stimulation, indicated a value of skull conductivity, σ_s, about 0.050 S/m. Hoekema et al. [3] have measured values in the range from 0.032 S/m to 0.080 S/m, taking great care to maintain their skull samples in normal *in vivo* conditions, e.g. in terms of temperature and fluid content, both of which they found to be important features. We also reported previously [7] that $\Delta<V_{ij}>_{stim}$ reached values of about 3 mV, both positive and negative. To assess the statistical significance of these results, we have calculated the error-normalized quantity $\Delta<V_{ij}>_{stim}/\delta\Delta_{ij}$ (denoted Δ/δ) for all experiments, and it is found to reach very high values, around 10 or 12, for a considerable number of cases. Fig. 2 shows an example for both volunteers under visual stimulation. Note that, for a single subject, these data are expected to be correlated via the field distribution.

To consider how the above voltage changes on stimulus might arise, calculations were performed using the methods and the simple concentric shell model of reference [2]. When the lower value of skull conductivity (0.006 S/m) was used, postulated changes of 1% in brain conductivity over a volume of 8 cm^3, due to stimulus, resulted in fractional changes in boundary voltage (compared with the homogeneous case) of 0.0001% to 0.01%; the results in [2]

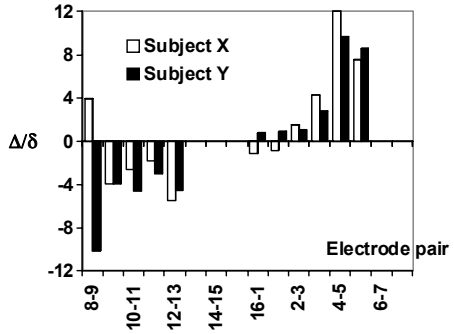

Fig. 2. Error-normalised voltage changes on visual stimulation, for current injection between electrodes 7 and 15.

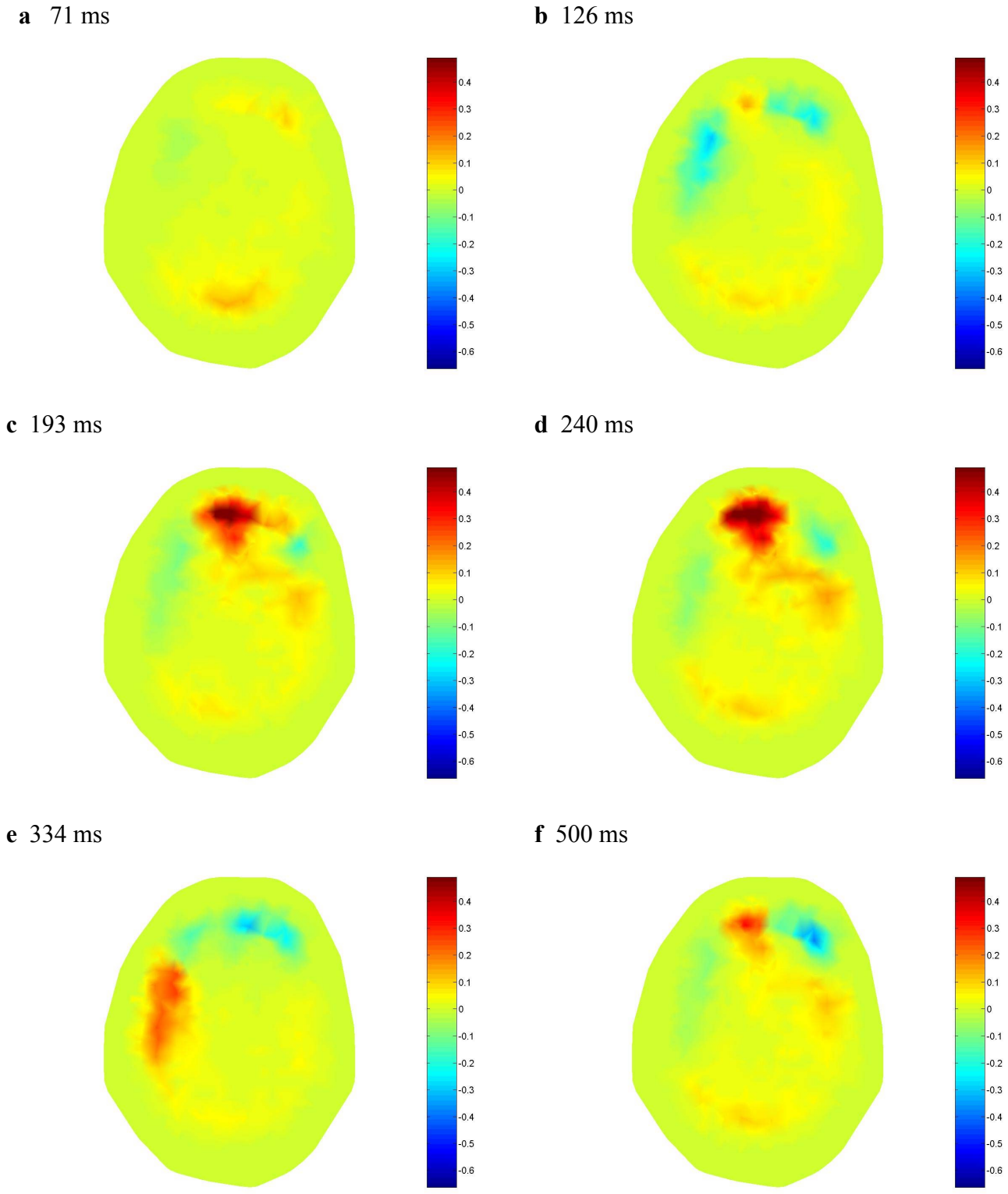

Figure 3 : Reconstructed imags of conductivity change (as a fraction of baseline conductivity) due to visual stimulus of one subject. The images include the scalp and the skull. The scale (right) is uniform for all images, as is the colour scale. The latency from flash to start of EIT data acquisition sequence is shown with each image.

show that this varies approximately linearly with both the conductivity change and the volume ('inclusion') over which it occurs. Hence, a conductivity increase of 15% over a 64 cm^3 volume, offset from the centre of the brain, yields fractional voltage changes ranging from 0.01% to 1%.

When $\sigma_s = 0.0533$ S/m is used in these calculations, the effect is to increase preferentially the lower range of the voltage changes by about a factor 10, whereas the larger fractional changes are increased by a factor of 2 to 3. For centrally-placed inclusions, where the largest amount of current flux is disturbed, there is again a disproportionate increase in the smaller values of fractional boundary voltage change values. Moreover, the largest *fractional* changes are predicted at the electrodes placed at 90 degrees to the line between the current-drive electrodes, an effect that we observe in our data. Conductivity changes of a few tens of percent within the inclusions are adequate to generate boundary voltage changes of 2 – 10%.

B. Images

Fig. 3 shows a few example images of $\delta\sigma$, in the electrode plane. The *variation* of $\delta\sigma$ within each image is the crucial and significant feature, rather than the absolute scale of $\delta\sigma$, given the need for calibration with representative "phantoms". The maximum value of $\delta\sigma$ within the images ranges up to about 40% for this volunteer. Typical data frames have about 40 "significant" singular values, relative to the Picard criterion. Hence, the spatial resolution of the images is approximately 2.5% of the cross-sectional area of the brain in the *superior putamen*. During visual stimulation, for both subjects X and Y, images acquired at latencies of 71 and 126ms post-flash (Fig. 3a, b), typically indicated an increase in conductivity towards the back of the brain, broadly corresponding with the areas V1, V2, V3 and V4 of the visual cortex. At 193 and 240ms for subject X only, increased conductivity was typically observed in (locations corresponding to) the right corpus callosum and the left anterior cingulate gyrus (Fig. 3c, d). In some frames for both subjects, increased conductivity in the left frontal regions was accompanied by decreased conductivity in the right frontal lobe (Fig. 3e). Conductivity changes often reduced to near-baseline levels in images acquired at 679ms. After repeated flash sequences, for both subjects, decreased conductivity at the right frontal lobe coincided with increased conductivity in the left anterior cingulate (Fig. 3f).

IV. DISCUSSION AND CONCLUSION

Measurements of rapid changes in resistance in cat visual and auditory cortex have been made by Klivington and Galambos [1], using electrodes inserted directly into the cortex to form an impedance arm within a Wheatstone bridge, excited at 10 kHz. For auditory and visual stimuli, electrical resistance shifts (ERS) were observed that had similar temporal characteristics to the usual evoked potentials (EPs). The ERS was typically 10 times greater than capacitive impedance variation. The ERS always showed, irrespective of brain location, a deep negative variation (w.r.t. baseline) lasting typically 10 – 20 ms, followed by a long period (e.g. 50 ms) of positive variation. The size of the ERS effect varied with intensity of stimulation in the same way as the EP. The ERS was much more sensitive than the EP to the level of barbiturate anaesthetic (ERS falls 70% when EP falls 10%). Klivington and Galambos considered the different possible mechanisms for the ERS and favoured those involving synaptic effects [1,9]. It is known [10] that barbiturate agents are effective on a specific GABA receptor subunit in the synaptic membranes. The evidence is thus overwhelming that the ERS is due to synaptic effects *in response to* neuronal discharge, rather than just the neuronal discharge itself. In the time domain, the images of conductivity change at early latencies shown in Fig. 3a and 3b correspond well with direct electrode recordings from visual interneurones in the macaque [6], ranging from 66ms for region V1 to 104ms for V4.

We conclude that the rapid EIT voltage changes in our data are due to synaptic effects, which result in changes of bulk conductivity in local brain tissue associated with neurological function. Hence, we conclude that the EIT images show the distribution of change in brain conductivity due to function.

REFERENCES

[1] K. A. Klivington and R. Galambos, "Rapid Resistance Shifts in Cat Cortex During Click-Evoked Responses," *J Neurophysiol*, vol. 31, no. 4, pp. 565-573, 1968.

[2] C.M. Towers et al., "3D Simulation of EIT for monitoring impedance variations within the human head", *Physiol. Meas.* Vol. 21, pp. 119-124, 2000.

[3] R. Hoekema et al., "Measurement of the Conductivity of Skull, Temporarily Removed During Epilepsy Surgery," *Brain Topogr.*, vol. 16, no. 1, pp. 29-38, 2003.

[4] A.T. Tidswell, A. Gibson, R.H. Bayford and D.S. Holder, "Three-Dimensional Electrical Impedance Tomography of Human Brain Activity", *Neuroimage* Vol. 13**,** pp. 283-294, 2001.

[5] D. Jancke, F. Chavane, S. Naaman, and A. Grinvald, "Imaging cortical correlates of illusion in early visual cortex," *Nature*, vol. 428, no. 6981, pp. 423-426, 2004

[6] M.T. Schmolesky et al. , "Signal Timing Across the Macaque Visual System," *J Neurophysiol*, vol. 79, no. 6, pp. 3272-3278, June1998

[7] J. C. Murrieta-Lee et al.,"Sub-second observations of EIT voltage changes on the human scalp due to brain stimulus", Proc. 26th IEEE Ann. Int. Conf. EMBS, pp. 1317-1320, San Francisco, CA, Sept. 2004

[8] N. Polydorides, W. R. B. Lionheart, and H. McCann, "Krylov subspace iterative techniques : On the detection of brain activity with Electrical Impedance Tomography," *IEEE Trans. Med. Im.*, vol. 21, pp. 596-603, 2002.

[9] K.A. Klivington, "Effects of pharmacological agents on sub-cortical resistance shifts", Exp. Neurol. Vol. 46, pp. 78-86, 1975.

[10] H. S. Lukatch and M. B. MacIver, "Synaptic mechanisms of thiopental-induced alterations in synchronized cortical activity," *Anesthesiology*, vol. 84, no. 6, pp. 1425-1434, 1996.